# Multicentre quantitative Ga-68 PET/CT performance harmonisation

Huizing, Daphne M. V.; Koopman, Danielle; van Dalen, Jorn A.; Gotthardt, Martin; Boellaard, Ronald; Sera, Terez; Sinaasappel, Michiel; Stokkel, Marcel P. M.; de Wit-van der Veen, Berlinda J.

*Published in:*
EJNMMI physics

*DOI:*
10.1186/s40658-019-0253-z

EJNMMI Physics

SHORT COMMUNICATION Open Access

# Multicentre quantitative $^{68}$Ga PET/CT performance harmonisation

Daphne M. V. Huizing[1], Daniëlle Koopman[2], Jorn A. van Dalen[3], Martin Gotthardt[4], Ronald Boellaard[5,6,7], Terez Sera[7], Michiel Sinaasappel[8], Marcel P. M. Stokkel[1] and Berlinda J. de Wit-van der Veen[1*]

* Correspondence: l.vd.veen@nki.nl
[1]Department of Nuclear Medicine, Netherlands Cancer Institute, Amsterdam, The Netherlands
Full list of author information is available at the end of the article

## Abstract

**Purpose:** Performance standards for quantitative $^{18}$F-FDG PET/CT studies are provided by the EANM Research Ltd. (EARL) to enable comparability of quantitative PET in multicentre studies. Yet, such specifications are not available for $^{68}$Ga. Therefore, our aim was to evaluate $^{68}$Ga-PET/CT quantification variability in a multicentre setting.

**Methods:** A survey across Dutch hospitals was performed to evaluate differences in clinical $^{68}$Ga PET/CT study protocols. $^{68}$Ga and $^{18}$F phantom acquisitions were performed by 8 centres with 13 different PET/CT systems according to EARL protocol. The cylindrical phantom and NEMA image quality (IQ) phantom were used to assess image noise and to identify recovery coefficients (RCs) for quantitative analysis. Both phantoms were used to evaluate cross-calibration between the PET/CT system and local dose calibrator.

**Results:** The survey across Dutch hospitals showed a large variation in clinical $^{68}$Ga PET/CT acquisition and reconstruction protocols. $^{68}$Ga PET/CT image noise was below 10%. Cross-calibration was within 10% deviation, except for one system to overestimate $^{18}$F and two systems to underestimate the $^{68}$Ga activity concentration. RC-curves for $^{18}$F and $^{68}$Ga were within and on the lower limit of current EARL standards, respectively. After correction for local $^{68}$Ga/$^{18}$F cross-calibration, mean $^{68}$Ga performance was 5% below mean EARL performance specifications.

**Conclusions:** $^{68}$Ga PET/CT quantification performs on the lower limits of the current EARL RC standards for $^{18}$F. Correction for local $^{68}$Ga/$^{18}$F cross-calibration mismatch is advised, while maintaining the EARL reconstruction protocol thereby avoiding multiple EARL protocols.

**Keywords:** Quantification, $^{68}$Gallium PET/CT, Image quality, Harmonisation

## Introduction

The use of $^{68}$Gallium ($^{68}$Ga)-labelled peptides for PET imaging has increased in the past years with the market authorisation for $^{68}$Ga/$^{68}$Ge-generators. The main applications include imaging of neuroendocrine tumours using somatostatin analogues and prostate cancer imaging using the prostate-specific membrane antigen [1, 2]. Though the interpretation of $^{68}$Ga-PET/CT is mainly based on visual assessment, quantitative measures should be used to evaluate or predict therapy response.

Previous experience with $^{18}$Fluorine ($^{18}$F) expressed the need for standardisation of acquisition and reconstruction protocols in order to retrieve comparable quantitative

imaging data. The EANM Research Ltd. (EARL) provides an accreditation programme to ensure PET/CT system harmonisation in multicentre $^{18}$F-FDG PET/CT studies [3]. This approach is based on standardizing the recovery coefficient (RC) for six phantom spheres with different sizes, thereby minimising inter- and intra-institute variability. For other isotopes, quantification should be evaluated separately as isotope characteristics can result in different image quality and quantification accuracy. For example, Makris et al. studied $^{89}$Zirconium ($^{89}$Zr) PET and showed the need for a specific harmonisation step including post-reconstruction smoothing to enable comparable quantitative measures among PET/CT systems [4]. In contrast, a recent $^{18}$F performance study showed that post-reconstruction filtering is not required for state-of-the-art PET/CT systems in relation to this isotope [5]. However, for $^{68}$Ga, such studies are not yet available.

In general, PET quantification accuracy depends on reconstructions, noise, and spatial resolution [6]. For $^{68}$Ga, the lower positron yield (89%), long positron range due to high initial positron energy (max 1.90 MeV, mean 0.84 MeV), short physical half-life (68 min) and small prompt gamma branching (3.2%, 1.077 MeV) may result in an inferior image quality compared to $^{18}$F [7]. Therefore, the aim of this study was to assess $^{68}$Ga-PET/CT quantification accuracy and reproducibility in a multicentre setting based on EARL standards.

## Materials and methods

### Clinical protocol evaluation

A survey among eight Dutch hospitals was performed to evaluate factors that affect quantification and to assess variability in clinical $^{68}$Ga-PET/CT acquisition protocols. Questions focussed on administered activity, PET/CT system, and acquisition- and reconstruction settings.

### $^{18}$F and $^{68}$Ga PET/CT phantom acquisitions

Eight European hospitals with 13 PET/CT systems performed phantom acquisitions, of which 11 systems were EARL accredited, but all had recoveries within the published EARL specifications. Six Biograph mCT systems (Siemens Healthineers, Erlangen, Germany), three Discovery systems (GE Healthcare, Milwaukee, WI, USA) and four Philips systems (Philips Healthcare, Eindhoven, The Netherlands) were included.

$^{18}$F and $^{68}$Ga acquisitions were performed at the end of 2017 and beginning of 2018 with two phantoms which were prepared using a standardised procedure by experienced staff from each centre. First, the NEMA PET cylindrical phantom was filled with 6–13 kBq/ml of $^{18}$F and $^{68}$Ga. Second, the NEMA NU-2 Image Quality (IQ) phantom was imaged using a 1:10 ratio with 2.0 and 20.0 kBq/ml of $^{18}$F and $^{68}$Ga in background compartment and spheres (37, 28, 21, 17, 13, and 10 mm diameter), respectively. Acquisitions of both phantoms were performed with minimal two bed positions and at least 5 min per bed position. Images were reconstructed according to local settings, including corrections for decay, randoms, dead time, CT-based attenuation, and scatter.

### Data analysis

Image noise was characterized for $^{68}$Ga only using the coefficient of variation (CoV) along a 30 × 30 × 160 mm bar in the centre of the cylindrical phantom.

Image quality was based on the RC of all six spheres, analysed by the EARL semi-automatic tool [5, 8]. The $RC_{max}$, $RC_{peak}$ and $RC_{mean}$ were determined as a function of sphere size based on the maximum voxel value ($RC_{max}$), the 1.0 $cm^3$ volume with the maximised average value ($RC_{peak}$) and the mean value of 50% isocontour of the maximum voxel value ($RC_{mean}$) with contrast correction, respectively. A spherical volume-of-interest (VOI) of ~ 300 ml in the centre of the cylindrical phantom and ten VOIs in the background of the IQ phantom were used for local PET and dose calibrator cross-calibration. IQ phantom background volume was 9400 ml, unless specified otherwise by the institute.

## Results

Eight Dutch hospitals provided their clinical acquisition- and reconstruction protocols (Table 1), which showed to be different.

An overview of all PET/CT systems and reconstruction settings is provided in Table 2. For local cross-calibration, most systems performed within 10% deviation of the dose calibrator (Fig. 1). The median [IQR] ratio was 0.93 [0.91–0.98] and

**Table 1** Acquisition and reconstruction settings of clinical $^{68}$Ga PET/CT imaging for prostate cancer and neuroendocrine tumours. One hospital per row is presented

| Site | PET/CT system | Reconstruction settings | Prostate cancer | | | Neuroendocrine tumours | | |
|---|---|---|---|---|---|---|---|---|
| | | | Minutes per bed position | | Injected activity | Minutes per bed position | | Injected activity |
| A | Philips Gemini TOF 64 | BLOB-OS-TF 4 mm 3i33ss | Pelvis: 4 | Body: 3 | 1.5 MBq/kg (range 50–250 MBq) | < 90 kg: 2.5 | > 90 kg: 3.5 | 2.6 MBq/kg (range 100–160 MBq) |
| B | Philips Gemini TF and XL | Astonish iterative reconstruction | 4 | | 2.0 MBq/kg | 4 | | 2.6 MBq/kg |
| C | Siemens mCT Flow | TrueX + TOF 2i21ss Gaussian 5mm | 1.5 mm/s CTM | | 2.0 MBq/kg | 2.5 | | 100 MBq |
| D | Philips Ingenuity TF | BLOB-OS-TF 4 mm 3i33ss 2 mm smooth B filter | NA | | | 4 | | < 90 kg: 150 MBq > 90 kg: 200 MBq |
| E | Siemens mCT TrueV | OSEM3D, TOF + PSF 2i21ss Gaussian 5 mm | 4 | | 1.5 MBq/kg (min 80 MBq) | NA | | |
| F | Philips Gemini TOF | BLOB-OS-TF 4 mm 3i33ss | Pelvis: 3 | Body: 2 | 100 MBq | 2.5 | | 100 MBq |
| G | Siemens mCT | TrueX + TOF 4i21ss Gaussian 5 mm | 3 | | 1.5 MBq/kg | 3 | | 1.5 MBq/kg |
| H | Siemens mCT40 and mCT128 | TrueX + TOF 3i21ss Gaussian 3 mm | < 70 kg: 1.5 MBq/kg: 3 1.13 MBq/ml: 4 0.9 MBq/ml: 5 | > 70 kg: 1.5 MBq/kg: 4 1.2 MBq/ml: 5 1 MBq/ml: 6 | 1.5 MBq/kg | < 70 kg: 1.5 MBq/kg: 3 1.13 MBq/ml: 4 0.9 MBq/ml: 5 | > 70 kg: 1.5 MBq/kg: 4 1.2 MBq/ml: 5 1 MBq/ml: 6 | 1.5 MBq/kg |

*NA* = not applicable, *i* = iteration, *ss* = subsets, *TOF* = time-of-flight, *PSF* = point-spread-function, *CTM* = continuous table motion

**Table 2** PET/CT reconstruction settings for phantom measurements

| No. | Manufacturer | PET/CT system | Reconstruction | Iterations | Subsets | Filter size (mm) | Matrix | Voxel size (mm) | Slice thickness (mm) |
|---|---|---|---|---|---|---|---|---|---|
| 1 | Siemens | Biograph mCT 40 (1) | PFS + TOF | 3 | 21 | 7.00 | 256 × 256 | 3.18 | 3 |
| 2 | Siemens | Biograph mCT 40 (2) | PFS + TOF | 3 | 21 | 7.00 | 256 × 256 | 3.18 | 3 |
| 3 | Siemens | mCT 123 X3R | Back projection | – | – | 5.00 | 200 × 200 | 4.07 | 5 |
| 4 | Siemens | Biograph mCT Flow 20 | PFS + TOF | 2 | 21 | 5.00 | 200 × 200 | 4.07 | 2.027 |
| 5 | GE | VCT | 3D IR† | NS | NS | NS | 128 × 128 | 5.47 | 3.27 |
| 6 | GE | Discovery D690 | VPFXS* | 4 | 8 | NS | 192 × 192 | 3.65 | 3.27 |
| 7 | Philips | Gemini TOF | BLOB-OS-TF | 3 | 31 | NS | 144 × 144 | 4 | 4 |
| 8 | Philips | Gemini TOF BigBore | BLOB-OS-TF | 3 | 31 | NS | 144 × 144 | 4 | 4 |
| 9 | Philips | Ingenuity | BLOB-OS-TF | 3 | 31 | NS | 169 × 169 | 4 | 4 |
| 10 | Philips | Vereos | BLOB-OS-TF | 3 | 15 | 3.00 | 144 × 144 | 4 | 4 |
| 11 | GE | Discovery 710 | VPFX§ | NS | NS | NS | 256 × 256 | 2.73 | 3.27 |
| 12 | Siemens | mCT 40 | PFS + TOF | 3 | 21 | 6.50 | 256 × 256 | 3.18 | 2 |
| 13 | Siemens | mCT 64 | PFS + TOF | 3 | 21 | 6.50 | 256 × 256 | 3.18 | 2 |

TOF or *TF* = time-of-flight, *PSF* = point-spread-function, *NS* = not specified
†3D OSEM
*3D OSEM with TOF and PSF
§3D OSEM with TOF

0.99 [0.97–1.01] for $^{68}$Ga and $^{18}$F, respectively. Two systems showed identical calibration accuracy for both isotopes (system 2 and 11), all other show a consistent underestimation for $^{68}$Ga. The $^{68}$Ga CoV in the centre of the cylindrical phantom was below 10% (Fig. 2).

The $^{18}$F RC-curves of all PET/CT systems satisfied the current EARL specifications (Fig. 3a–c). However, for $^{68}$Ga the RC-curves were located around the lower limit of the EARL specifications (Figure 3d-f). In addition, $^{68}$Ga showed a reduced mean recovery and larger variation between PET/CT systems compared to the $^{18}$F. The variation for all spheres of the $RC_{mean,}$ $RC_{max}$ and $RC_{peak}$ for $^{18}$F was 6%, 6% and 8%, respectively. For $^{68}$Ga, the mean range was 11%, 11% and 15% (largest variation was 19%). Furthermore, the mean $RC_{max}$ and $RC_{mean}$ were both 11% lower compared to the mean EARL specifications for $^{18}$F. The mean $^{68}$Ga/$^{18}$F calibration difference within one scanner was 7% (range 1–13%).

After correction for the local difference between $^{68}$Ga/$^{18}$F cross-calibration (Fig. 1), the $^{68}$Ga RC curve was within EARL limits for all but two scanners (Figure 4). The mean $^{68}$Ga $RC_{max}$ and $RC_{mean}$ were accordingly 5% lower compared to mean EARL standards.

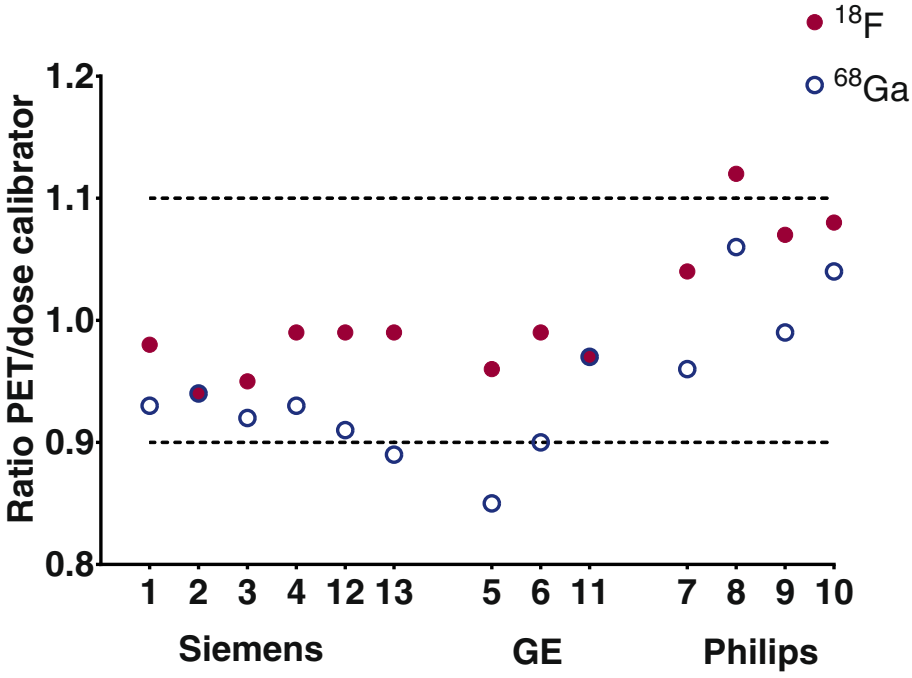


**Fig. 1** Accuracy of the measured activity by the PET/CT system and local dose calibrator, based on the average between the cylindrical and IQ phantom. Numbers correspond to Table 2

## Discussion

In this study, quantitative $^{68}$Ga PET/CT performance was evaluated in a multicentre setting. In a survey across Dutch hospitals, differences in clinical acquisition and reconstruction protocols were observed, underlining the need for clinical harmonisation. Although 11 out of the 13 PET/CT systems were EARL accredited, all systems showed

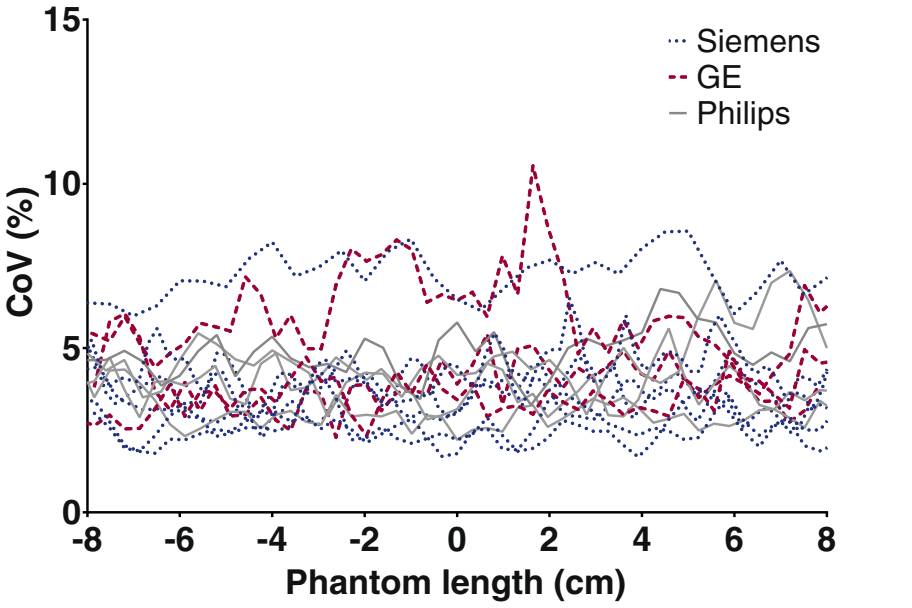


**Fig. 2** Noise across the cylindrical phantom filled with $^{68}$Ga, visualized as coefficient of variation (CoV)

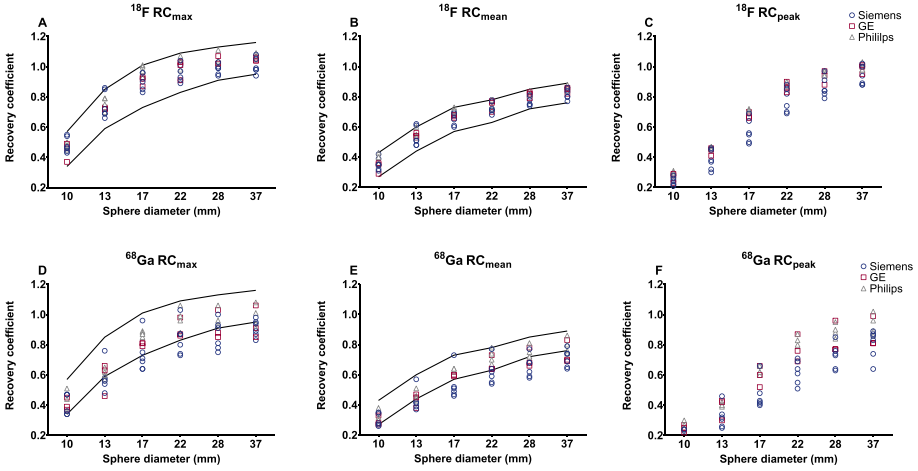


**Fig. 3** RC for $^{18}$F with the current EARL standards and RC of $^{68}$Ga. Solid lines: maximum and minimum values according to EARL limits as applicable before 2019

$^{18}$F recovery performance within EARL standards. For this reason, all systems were included for $^{68}$Ga evaluation.

The absence of local and central dose calibrator cross-calibration for $^{68}$Ga is a limitation in this study. This would increase local calibrator harmonisation and improves PET/CT comparability across sites. Most institutes use a long-lived ($^{137}$Ceasium) source to assess constancy and accuracy of the dose calibrator on a daily basis, and perform actual cross-calibration with the PET/CT system at least once a year using $^{18}$F. Still, in all but three PET/CT systems the measured $^{18}$F and $^{68}$Ga activity concentrations were within 10% deviation from the local dose calibrator. High energy prompt gammas emitted by $^{68}$Ga are likely detected by the dose calibrator causing a disconcordance, yet in fewer extent by the PET system. Because of this, the dose calibrator overestimates $^{68}$Ga-activity, and a persistent underestimation for $^{68}$Ga compared to $^{18}$F is seen in Fig. 1. A recent study by Bailey et al. also showed an underestimation of ± 15% for $^{68}$Ga, which was primarily related to an inaccurate scaling factor for the dose calibrator of a specific vendor [9]. To avoid these issues, they calibrated the dose calibrator towards the PET, after verifying that the scanner has a good response for $^{18}$F. These results are also supported by the fact that on specific Siemens scanners (scanners 1 and 2), a traceable $^{68}$Germanium ($^{68}$Ge) source was used to verify absolute PET response independent of a dose calibrator. When imaging the $^{68}$Ge-source, the PET/

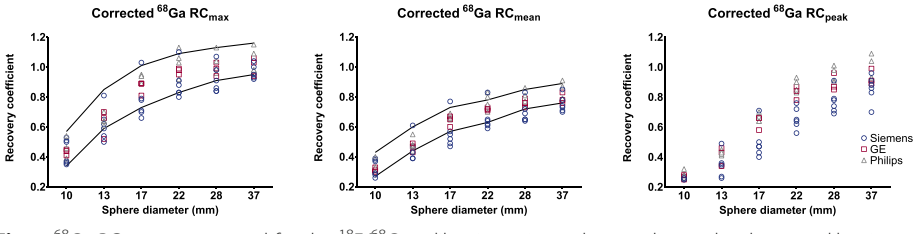


**Fig. 4** $^{68}$Ga RC-curves corrected for the $^{18}$F/$^{68}$Ga calibration mismatch according to local cross-calibration. Solid lines: maximum and minimum values according to EARL limits as applicable before 2019

CT system did not show the same offset as was observed when imaging the $^{68}$Ga cross-calibration phantom (roughly a deviation of < 1% vs. 6% and 7%, respectively). For the sake of simplicity, we would suggest to correct the RC curve for the local $^{68}$Ga/$^{18}$F discrepancy, as after correction for this $^{68}$Ga/$^{18}$F difference (Fig. 4) all but two scanners were within EARL specifications. This correction has to be performed offline in multicentre quantitative studies. The $^{68}$Ga used for this study was produced either locally or by a pharmaceutical institution and was therefore not traceable to a central dose calibrator. We expect that the response between the dose calibrator and the PET-system could be uniform in future clinical $^{68}$Ga-PET/CT studies if a traceable (NIST) source is used to harmonise protocols between centres.

$^{68}$Ga image noise was below 10% for all PET/CT systems which is in concordance with the EANM/EARL guidelines [3, 8]. The RC variation is larger for $^{68}$Ga compared to $^{18}$F (Fig. 3). However, $^{68}$Ga performance nearly reached EARL performance specifications after correction for the local $^{68}$Ga/$^{18}$F ratio. Surprisingly, the $RC_{peak}$ variation (8% and 15%) is larger in contrast to $RC_{max}$ and $RC_{mean}$ (both 6% and 11%) for both $^{18}$F and $^{68}$Ga, respectively. The study of Kaalep et al. showed the opposite result in $RC_{peak}$ variation [5]. The $RC_{peak}$ is expected to be less prone to noise compared to $RC_{max}$; therefore, it was expected to be more comparable over all PET-systems. The difference could be explained by the fact that the standard deviation of $RC_{max}$ and $RC_{peak}$ are similar: 8.4% and 8.6% for $^{68}$Ga and 4.8% and 5.0% for $^{18}$F, respectively. Yet, the mean $RC_{peak}$ value is lower; therefore, resulting in a higher CoV. Next to that, the larger $^{68}$Ga variation in the RC-curves compared to $^{18}$F is likely related to the higher positron energy of $^{68}$Ga and thereby revealing a lower signal-to-noise ratio. This effect is enhanced by post-reconstruction filtering. Finally, previous single-centre studies show $^{68}$Ga RC-curves similar [10] or somewhat better due to point spread function reconstruction [11] as observed in the current study. The EARL limits as applicable before 2019 (EARL1) are shown in Figs. 3 and 4, as all acquisitions were acquired before 2019 and therefore site-specific acquisition and reconstruction protocols are designed to meet the EARL1 limits. $RC_{peak}$ specifications are not available for EARL1 and are therefore not shown in Figs. 3 and 4. EARL2 limits (applicable from 2019) for $RC_{max}$ and $RC_{mean}$ increased with ~ 25% in comparison to EARL1. We expect that the gap between $^{18}$F and $^{68}$Ga recoveries will further increase with these new limits, as already for EARL1 not all scanners agreed to EARL1 limits after $^{68}$Ga/$^{18}$F correction (Fig. 4).

Based on the results, we propose to correct $^{68}$Ga recovery towards the $^{18}$F recovery to correct for the current dose calibrator deviation. We suggest, therefore, to apply the EARL acquisition and reconstruction protocol and to correct for $^{68}$Ga/$^{18}$F cross-calibration mismatch. One can assume that $^{68}$Ga recovery is steady if $^{18}$F specifications of a PET-system are stable during regular yearly assessment. Unless the acquisition and reconstruction protocol is changed or major maintenance is performed to the PET/CT-system, we recommend to perform additional $^{68}$Ga IQ acquisitions only when regular $^{18}$F evaluations are deviating. An EARL accreditation programme for $^{68}$Ga can thus be based on the $^{18}$F accreditation but extended with a cross-calibration verification between $^{68}$Ga measured by the dose calibrator and PET/CT system only, similarly as proposed by Kaalep et al. for $^{89}$Zr [12]. In addition, frequent $^{18}$F cross-calibration acquisitions using the cylindrical phantom are advised, especially after PET/CT system maintenance.

## Conclusion

This evaluation of multicentre $^{68}$Ga PET/CT performance showed that $^{68}$Ga RCs perform at the lower limits of current $^{18}$F EARL standards. For practical reasons, we recommend to use the $^{18}$F EARL approved reconstruction settings and to correct for $^{68}$Ga/$^{18}$F calibration mismatch based on local cross-calibration. Finally, we suggest to evaluate $^{68}$Ga PET/CT recovery performance once and repeat only when $^{18}$F specifications are changed.

### Abbreviations

$^{18}$F: $^{18}$Fluorine; $^{68}$Ga: $^{68}$Gallium; $^{89}$Zr: $^{89}$Zirconium; CoV: Coefficient of variation; EARL: EANM Research Ltd; IQ: Image quality; RC: Recovery coefficient; VOI: Volume-of-interest

### Acknowledgements

The authors thank A. Eek for coordinating the BetaCure study. Furthermore, we thank the hospitals of the Dutch PSMA consortium and the other centres who have sent their clinical $^{68}$Ga PET/CT acquisition protocols.

### Authors' contributions

DH performed data collection, analysis and drafted the manuscript. DH, DK, LWV, MS and JvD discussed the methodology. RB provided the analysis tools and discussed methodology. All authors critically reviewed the manuscript and approved the final version of the manuscript.

### Funding

The research leading to these results have received funding from the European Community's Seventh Framework Programme (FP7/2007-2013) under grant agreement no. 602812 (BetaCure study).

### Availability of data and materials

The datasets used and/or analysed during the current study are available from the corresponding author on reasonable request.

### Ethics approval and consent to participate

This article does not contain any studies with human participants or animals performed by any of the authors.

### Consent for publication

Not applicable.

### Competing interests

RB is a scientific advisor and chair of the EARL accreditation programme. TS is an associate of the EARL accreditation programme. All other authors declare that they have no conflict of interest.

### Author details

[1]Department of Nuclear Medicine, Netherlands Cancer Institute, Amsterdam, The Netherlands. [2]Department of Nuclear Medicine, Isala, Zwolle, The Netherlands. [3]Department of Medical Physics, Isala, Zwolle, The Netherlands. [4]Department of Radiology and Nuclear Medicine, Radboud University Medical Center, Nijmegen, The Netherlands. [5]Department of Radiology and Nuclear Medicine, Amsterdam University Medical Centres, location VU University Medical Center, Amsterdam, The Netherlands. [6]Department of Nuclear Medicine and Molecular Imaging, University of Groningen and University Medical Center Groningen, Groningen, The Netherlands. [7]EANM Research Limited (EARL), Vienna, Austria. [8]Department of Physics, Netherlands Cancer Institute, Amsterdam, The Netherlands.

Received: 3 May 2019 Accepted: 2 September 2019
Published online: 08 November 2019

### References

1. Singh S, Poon R, Wong R, Metser U. $^{68}$Ga PET imaging in patients with neuroendocrine tumors: a systematic review and meta-analysis. Clin Nucl Med. 2018;43:802–10.
2. Lütje S, Heskamp S, Cornelissen AS, Poeppel TD, van den Broek SAMW, Rosenbaum-Krumme S, et al. PSMA ligands for radionuclide imaging and therapy of prostate cancer: clinical status. Theranostics. 2015;5:1388–401.
3. Boellaard R, Willemsen A, Arends B, Visser EP. EARL procedure for assessing PET/CT system specific patient FDG activity preparations for quantitative FDG PET/CT studies. 2013. p. 1–3. Available from: http://earl.eanm.org/html/img/pool/EARL-procedure-for-optimizing-FDG-activity-for-quantitative-FDG-PET-studies_version_1_1.pdf.
4. Makris NE, Boellaard R, Visser EP, de Jong JR, Vanderlinden B, Wierts R, et al. Multicenter Harmonization of $^{89}$Zr PET/CT Performance. J Nucl Med. 2014;55:264–7.
5. Kaalep A, Sera T, Rijnsdorp S, Yaqub M, Talsma A, Lodge MA, et al. Feasibility of state of the art PET/CT systems performance harmonisation. Eur J Nucl Med Mol Imaging. 2018;45:1344–61.
6. Boellaard R, Krak NC, Hoekstra OS, Lammertsma AA. Effects of noise, image resolution, and ROI definition on the accuracy of standard uptake values: a simulation study. J Nucl Med. 2004;45:1519–27.
7. Sanchez-Crespo A. Comparison of Gallium-68 and Fluorine-18 imaging characteristics in positron emission tomography. Appl Radiat Isot. 2013;76:55–62.

8. Boellaard R, Delgado-Bolton R, Oyen WJG, Giammarile F, Tatsch K, Eschner W, et al. FDG PET/CT: EANM procedure guidelines for tumour imaging: version 2.0. Eur J Nucl Med Mol Imaging. 2015;42:328–54.
9. Bailey D, Hofman M, Forwood N, O'Keefe G, Scott A, van Wyngaardt W, Howe B, Kovacev O, Francis R. Accuracy of dose calibrators for $^{68}$Ga PET imaging: unexpected findings in a multicenter clinical pretrial assessment. J Nucl Med. 2018;59:636–8.
10. Preylowski V, Schlögl S, Schoenahl F, Jörg G, Samnick S, Buck AK, et al. Is the image quality of I-124-PET impaired by an automatic correction of prompt gammas? PLoS One. 2013;8:1–8.
11. Jönsson L, Stenvall A, Mattsson E, Larsson E, Sundlöv A, Ohlsson T, et al. Quantitative analysis of phantom studies of $^{111}$In and $^{68}$Ga imaging of neuroendocrine tumours.
12. Kaalep A, Huisman M, Sera T, Vugts D, Boellaard R. Feasibility of PET/CT system performance harmonisation for quantitative multicentre $^{89}$Zr studies. EJNMMI Phys. 2018;5:26.

## Publisher's Note